INDEXCUB: A READY-TO-USE SET OF ROUTINES FOR X-RAY DIFFRACTION LINE PROFILE ANALYSIS

Adriana Pérez-Casanova, Héctor Medel-Cobaxin and Flavio F. Contreras-Torres*
Escuela de Ingeniería y Ciencias, Tecnológico de Monterrey, Monterrey 64849, Mexico
*corresponding author: contreras.flavio@tec.mx

ABSTRACT
The growing interest in the use of powder X-ray diffractometry for materials characterization has led to the introduction of relevant concepts (e.g. microstructure, strain, anisotropy, texture) to undergraduate teaching in engineering and science. In this concern, the study of polycrystalline materials underlays the use of appropriate software: free, licensed, proprietary or commercial to assist research on structure determination, structure refinement, and microstructure characterization. Today with the easy accessibility to personal computers, routines for powder diffractometry becomes also feasible for non-specialist. Therefore, it would be relevant that students with computing knowledge may decide to improve routines on such three tasks incorporating their own computational approaches. In this study, we show the development of a ready-to-use and open source program written in GNU-Octave (v4.2.1) focused on X-ray diffraction line-profile analysis. The programing language platform was chosen mainly due to two reasons: (1) there is no requirement for commercial licenses, meaning that both programing language and routines can be downloaded online, facilitating collaborative efforts between students, instructors and developers, and (2) easy re-coding of evaluation strategies is always allowed though fast implementation of modules into the code. The code, IndexCub, features routines for background subtraction, whole profile smoothing and $K\alpha_2$ radiation removal, location of diffraction peaks positions, indexing for cubic specimens, multi peak separation of individual peaks, and evaluation of full width at half-maximum and integral breadth values. Microstructure properties are characterized through of integral breadth methods (e.g. Williamson-Hall) and Fourier analysis (e.g. Warren-Averbach), and the anisotropy effects are incorporated introducing calculations of contrast factors. In terms of diffraction domain sizes, size distribution and the lattice microstrain, the analysis of the microstructure is discussed along with examples for polycrystalline coarse-grained materials (NaCl), epitaxial film (Si), and thin-films (Au) specimens. The code facilitates the understanding of microstructure analysis by using theoretical approaches well established and in state-steady level.

Keywords: X-ray diffraction; microstructure; polycrystalline powders; thin-films.

INTRODUCTION
Polycrystalline materials are solids (e.g., powders, compact bulk materials, ceramics, ionic crystals, metals) deviating from a perfectly ordered structure to form small crystalline domains, which are all contained into grains or particles. The grain size may range from a few to ten of microns. A special class of polycrystalline materials feature grain size less than 100 nm and a high density (10^{19} per cm^3) of grain boundaries; this class is called nanocrystalline materials (Gleiter, 2000). Thin-films (less than 1 μm in thickness) can be classified as epitaxial (single crystal), polycrystalline, or amorphous materials depending on homogeneity in crystalline domains. Catalytic converters, self-cleaning surfaces, magnetic nanostructures, supra-hard

This document was presented at the Denver X-ray Conference (DXC) on Applications of X-ray Analysis.

Sponsored by the International Centre for Diffraction Data (ICDD).

This document is provided by ICDD in cooperation with the authors and presenters of the DXC for the express purpose of educating the scientific community.

Usage is restricted for the purposes of education and scientific research.

DXC Website
– www.dxcicdd.com

ICDD Website
- www.icdd.com

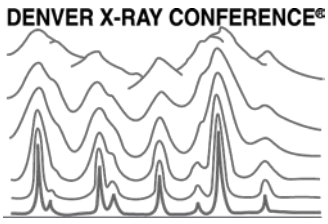

composites, among others, are great examples of polycrystalline materials in technological applications (Suryanarayana, 1995).

In the study of polycrystalline materials, a reliable technique for specimen microstructural characterization is transmission electron microscopy (TEM) and high-resolution TEM (Kril and Birringer, 2009). However, it may became demanding to carry out several evaluations for a series of specimens prepared under different experimental conditions as well as subsequent heated treatments, plastic deformations, doping, sintering, etc. In addition, the information obtained using TEM is local and may not represent the average properties. X-ray diffraction (XRD) technique is a suitable alternative because it usually examines 10^3–10^5 larger sample volume than that studied by TEM. Therefore, XRD can offers the advantages of being fast in obtaining a truly statistically averaged information of the specimen, easy preparation of the sample, non-destructive method, and low-cost of maintenance (Snyder *et al.*, 1999). XRD is also a very valuable tool in undergraduate programs for developing interests in analytical methods, instrumentation and routing code development (Jenkins, 2001; Butera and Waldeck, 1997; Pope, 1997; Ryan, 2001; Stojilovic, 2018).

XRD has became a standard technique in many laboratories, it is employed mainly for qualitative analysis and phase identification through comparison between experimental data and files of reference patterns. To this comparison, the overall methodology for checking single-phase data files is the Rietveld method, in which structural parameters and other instrument effects are refined to match measured data. A second group of analysis is concerned with a structure determination by powder diffractometry (SDPD) for indexing powder patters. This task is commonly explored through trial-and-error, dichotomy and Monte Carlo approaches. While several programs have appeared on the market to carry on both Rietveld and SDPD routines, there is a third group of methods less spread into the powder diffraction community. This is the group of methods focused on the study of the microstructure properties, namely, crystallite size, size distribution, stacking faults, twin boundaries, dislocations, chemical heterogeneities, vacancies, surface relaxation. Therefore, it would seem that activities for determining particular microstructure parameters from XRD line profiles is often missing in undergraduate programs. So far, the Scherrer equation is traditionally used to approach the crystallite size, which in fact is frequently overestimated as it does not take into account to the presence of sample micro-strain. The procedure of the evaluation of the peak profiles for microstructure analysis is referred to as X-Ray line profile analysis, XLPA (Gubicza, 2014). XLPA methods are suitable to introduce anisotropic effects from fundamental approaches, and thus evaluate X-ray peak broadening as a correlation between crystallite size and lattice strain. Comparing with Rietveld, XLPA methods determine parameters by fitting theoretical functions on the line profiles (i.e., not necessary a reference pattern). In this study, ready-to-use coding routines incorporate methodologies of line-broadening analysis to evaluate coherent diffraction domain sizes, size distribution and lattice microstrain. The objective is to present a set of functions introducing specific methods for handling XRD current problems in the processing X-ray line profiles of experimental data. The bases for the methods to be discussed have been reported previously, and today constitute well established data processing routines and in state-steady level. In a first approach, the set of routines process XRD data from grains (NaCl), and epitaxial (Si) film and thin-films (Au sputtered from radiofrequency). Undergraduate students of chemistry, physics and nanotechnology programs can promptly learn how to apply a set of functions to create own

custom scripts to improve their skills in the microstructural characterization of polycrystalline materials through of XLPA.

IMPLEMENTATION

Several routines and computer programs to carry out the analysis for powder diffraction have been published elsewhere (Cranswick, 2008). A short list of computational contributions to XLPA is described in Table 1.

Table 1.

Code	Year	Developers	Language
N.N.	1966	Hoff and Kitchingman	Atlas
N.N.	1969	Ungár	ICT-Algol
N.N.	1971	Schramm	Fortran
WPPF	2001	Scardi and Leoni	Fortran
MWP-fit	2001	Ribárik, Ungár, and Gubicza	C
WPPM	2002	Scardi and Leoni	Fortran
ANIZC	2003	Borbély, Dragomir-Cernatescu, Ribárik and Ungár	C
PM2K	2006	Leoni, Confente and Scardi	C++
MStruct	2008	Matej, Nichtová and Kuzel	C++/Matlab
N.N.	2009	Martinez-Garcia, Leoni, Scardi	Matlab
N.N.	2014	de Rooi, van der Pers, Hendriks, et al.	Matlab
DIPPA	2016	Simm	Matlab

In this study, we show a set of routines written in GNU-Octave (v4.2.1) programming language to carry out the pretreatment of XRD data and further study of microstructure. The set is divided into routines according to the procedures described below. GNU-Octave is chosen for the organization, storage and analysis of data because this programing language has the capacity to import data from a variety of sources (*.xy, *.dat, *.txt), store the data in arbitrarily data structures (i.e. it can handle easily, compactly and quickly both vector and matrixes), manipulate such data using built-in and user defined functions. All output data can be tabulated, and figures can be plotted in the same GUI platform.

Background

XRD background arises from a number of sources, including, fluorescent radiation and incoherent scattering from the specimen, diffraction of the continuous spectrum, collimator, air, etc. The accurate determination of the diffraction peak properties (e.g., height, integrated intensity, integral breadth, centroid, variance, fourth moment and the Fourier coefficients of the line profile) depends to various extents on an estimation of the background (Mitra, 1966). For instance, XLPA is more repeatable if background has been previously eliminated from the data. The criterion for accepting a peak representing a true X-ray diffraction line would require the peak to be higher than 3-5 standard deviations above background. Two basic algorithms to estimate the background are employed in common programs. The first method uses a predetermined background model and simply adjusts an additive constant. At first, a background intensity is just being user-selected representing a constant count level defined to the entire range of the diffractogram. Anything upper would be considered as a peak including those noise points that surpass the level. Alternatively, the background can be represented through selected points that will be used to model a much more complex function. The intensities of the first and last

points (about 100 points) can be selected for drawing a straight line (i.e., the background) though the averaged values. Thus, the background intensity at a point $2\theta_i$ can be calculated easily as:

$$\mathrm{bkgl_i} = \left(\frac{z-a}{2\theta_N - 2\theta_1}\right) 2\theta_i + \frac{a(2\theta_N) - z(2\theta_1)}{2\theta_N - 2\theta_1}$$

where, $z = 1/N \sum I(2\theta_i)$ and $a = 1/N \sum I(2\theta_{N-i})$ are the averaged last and first *N* points selected.

The second method, which we are referring in this paragraph, uses polynomial approaches. Typically, the background is a collection of points, which can be represented by a smoothing curve using polynomials. The first approximation is the method called *cubic splines*, which consists of a construction of curves through piecewise cubic polynomials (i.e., functions numerically well behaved that support inflections). To this, pairs of control points represent short segments of the curve. The solution of coefficients requires conditions of continuity at the joints, slope and curvature constrains, and limits at the borders to represent a set of linear equation and its solution $\mathbf{a} = \mathbf{M}^{-1}\,\mathbf{y}$, where the vector **a** contains the corresponding coefficients polynomials.

In order to have local shape control, *Hermite cubic splines* are employed when parametrizing over tight portions of curves. To this is required slopes in parametric form at each control point. The control points are obtained from raw data for which two-theta and intensity (y_0) values are arranged as vectors. Ideally, these pairs should be taken automatically, i.e., without the user having to select segments of the pattern. The first step obtains the indexes for all points y_0 that are located at a certain background level. The resulting polynomial background coefficients are saved in the directory where the raw data is located allowing to judge the fit and adjust their model or starting parameters accordingly.

Profile smoothing

To reduce random noise for a series of counts, the most generalized method in the literature is the Savitzky and Golay smoothing method (Savitzky and Golay, 1964). This filter was initially used for spectral lines in noisy spectrometric data, but promptly was adopted in other physical processes in which the enhancement of signal-to-noise ratios is also relevant. The original algorithm has been modified to get better local estimates of the expected values (Luo *et al.*, 2005; de Rooi, 2014).

Considering a successive subset of $2m + 1$ points that are going to be fitted by a smooth series μ, represented as a polynomial of degree k in j (with $k \leq 2m$) and with the same length of the selected points, then such a series μ and its nth derivative can be represented by:

$$\mu_j = \sum_{k=0}^{k=n} b_{n,k} j^k = b_{n,0} + b_{n,1} j^1 + b_{n,2} j^2 + \cdots + b_{n,n} j^n$$

$$\frac{d^n \mu_j}{dj^n} = n!\, b_{n,n}$$

The coefficients $b_{n,n}$ are to be selected in such a way that when each *j*-point data (abscissa) is substituted into μ_j, then the sum of the squares of the differences between the computed values (μ_j) and the observed values (y_j) requires be a minimum over the interval being considered. Thus, the *least-squares* criterion is used to measure the fit,

$$\frac{\partial}{\partial b_{n,k}}\left[\sum_{j=-m}^{j=m}\left(\mu_j - y_j\right)^2\right] = 0$$

If a minimization is considered with respect to the *r*th differentiation

$$2\sum_{j=-m}^{j=m}\left[\left(\sum_{k=0}^{k=n} b_{n,k} j^k\right) - y_j\right] j^r = 0$$

The running least-squares polynomial fitting can be automatically performed by convolving the entire input data with a digital filter. The running equation is as follows,

$$\sum_{k=0}^{k=n} b_{n,k}\, S_{r+k} = F_k$$

where $S_{r+k} = \sum j^{r+k}$ and $F_k = \sum j^k y_j$. In principle, the convolution coefficients are obtained for all data points, all polynomial degrees and all differentiation orders.

IndexCub uses routine that performs smoothing with an algorithm based on the method published by de Rooi *et al*. (2014) showed a penalized likelihood smoothing approach. The line-profile is mathematically smoothed by least-squares fit of a series (i.e. polynomial) of points that does not deviate too much of the original data and without loss of resolution. Such a strategy provides the possibility of using *n*th-order decomposition on the experimental data. Taking advantage of a simple averaging of a large number of counts, at first the noise is reduced as the square root of the number of "points". Then it can sometimes be useful to replace each data point by some kind of local average of surrounding data points.

Kα$_2$ radiation removal

In comparison with single crystals, which show narrow diffraction peaks, polycrystalline specimens diffracted showing peak not only broadened but also containing doublets. The origin of these doublets comes from X-ray tube sources, which give radiation beyond the simple Kα emission required for diffraction measurements. This additional radiation includes other emission lines from the anode, including a strong Kβ emission, and emission lines from tube impurities such as tungsten, arising from the tube cathode. While physical filtering or monochromators are used to reduce Kβ radiation, computational routines subtract Kα$_2$ radiation.

A classical routine for stripping Kα$_2$ radiation is based on the Rachinger correction (Rachinger, 1948). This graphical approach assume that the peak shape is the same for Kα$_1$ and Kα$_2$, and that

α_2 line is expected to be half the intensity of α_1. The intensity of the diffraction profile can be represented by

$$I(2\theta_i) = I_{\alpha 1}(2\theta_i) + \frac{1}{2} I_{\alpha 1}(2\theta_i - d)$$

where $d = 2\theta_{\alpha 2} - 2\theta_{\alpha 1}$ is the doublet separation, a known function of the diffraction angle 2θ and wavelengths that can be determined using the Bragg equation $\lambda = 2d \sin\theta$, thus the distance is calculated as

$$d = 2\left[\arcsin\left(\frac{\lambda_2}{\lambda}\sin\theta\right) - \arcsin\left(\frac{\lambda_1}{\lambda}\sin\theta\right)\right]$$

Because the doublet distance *d* does not coincide with the data points, it is necessary to use models that allows interpolation. A simple model assumes a straight line in the range

$$2\theta_j \leq 2\theta_i - d \leq 2\theta_k$$

However, this approach yields to results that became asymmetrical on the high-angle side of the diffractogram. A much more sophisticated approach (de Rooi, 2014) uses the principle that the X-ray photons counts follow a Poisson distribution, which is assumed binomial on the log scale. To this, the penalized composite link model (PCLM) proposed by Eilers (2007) and smoothing the counts by B-splines bases on a regular grid, combined with a penalty.

Peak search

Angular locations on the whole profile line are employed to attribute the position and intensities of peaks. IndexCub incorporate a routine that is able to find and select peaks above a background level. To this, the routine obtains the first derivative of the whole profile previously smoothed using central-difference approaches, and then it takes only those downward-going zero-crossings values as truly diffraction peaks. To avoid problems in searching, the routine use two main parameters to raise a slope at the angular location where the original point exceeds a certain amplitude threshold.

Indexing

Indexing powder diffraction patterns consists in the determination of the unit cell by assigning Miller indices to each reflection. IndexCub is focused mainly to index a diffraction patterns from cubic materials corresponding to simple cubic (SC), body-centered cubic (BCC), face-centered cubic (FCC), or diamond cubic (DC). The sample has to correspond to a single phase. A standard procedure determines the structure using an iterative process based on trial-and-error approach described by Werner *et al*. (1985). For each peak, the interplanar spacing (d_{hkl}) is calculated form basic equations and employed for further indexing in the form of

$$Q = a_{11}h^2 + a_{22}k^2 + a_{33}l^2 + a_{12}h \cdot k + a_{23}k \cdot l + a_{13}h \cdot l$$

where $Q = 1/d_{hkl}^2$ and a_{ij} represents a set of reciprocal-cell relationships. For each a_{ij} value there is a linear system $\mathbf{MA} = \mathbf{Y}$ where **M** is a square matrix of Miller indices, **Y** is a vector that represents the set of observed *Q* values (i.e. diffraction lines), and **A** is the unknown parameter set for a_{ij} values containing the proposed unit-cell parameters. The trial-and-error paradigm

calculates theoretical position of Miller indices and compares with those from the observed lines until defined criteria are satisfied. The number of trials depend on the *hkl* triples, and unit-cell parameters.

FWHM and integral breadth

The width of diffracted peaks are described by full width at half-maximum (FWHM) using a linear interpolation method. On the other hand, a routine based on a trapezoidal method calculates the integral breadth values, β, which is defined as the ratio of the peak area and peak maximum. In particular, β (in the units of the reciprocal space, 1/*d*) values are preferred due to they are less dependent on the shape of the peaks. IndexCub carry out a procedure for $K\alpha_2$ elimination prior to obtain values of FWHM and β.

Line profile analysis

Screw dislocations and twin boundaries are structural defect that cause microstrain. Typically, it yields in broadening of peak profiles. Lattice strain or microstrain is a local deviation of *d*-spacing values instead of peak shift. The *d*-spacing is contracted or expanded accordingly around the defect. The origin may be point defects like interstitial or missing atoms, or substitution with different atoms. Both size and strain broadening affect the width of diffraction peaks; however, this parameters show a different angular dependence of the peak width. There is two common ways to assess these defects, namely, integral breadth methods and Fourier analysis.

Integral breadth methods: The integral breadths (β_{hkl}) values of individual *hkl*-reflections are determined as a function of the projection of diffracting planes. These integral breadth values can be plotted to observe if there exists a trend that monotonically be depended on such projection. The most broadened indicates that the crystallite is truncated in such reflections on those [*hkl*] directions. IndexCub is able to model the peak profile by a Gauss, Cauchy or pseudo-Voight function in units (δ2θ units). If the profile is assumed to be Cauchy, the following relationship holds $\beta^* = 1/\tau + 2\zeta d^*$, and where $d^*=(2\sin\theta)/\lambda$ is the inverse of the scattering vector, ζ and τ are the apparent strain and sizes, respectively. Finally, the broadening profiles can also be approximated by Gaussian functions.

IndexCub also incorporates Williamson-Hall plots to describe basic features of line broadening (e.g., source of broadening and line broadening anisotropy) in which either size or strain effects are clearly dominating (Cavazos-Cavazos and Contreras-Torres, 2017). Despite the fact that the derivation of the Williamson-Hall method explicitly assumes purely Cauchy broadening, which is often not fulfilled in reality, the routines are able to assume Gauss function to carry put WH analysis.

Fourier analysis. Discrete Fourier Transformations are performed to carry out Warren-Averbach analysis. IndexCub incorporate DFT considering the experimentally measured peaks (i.e. the profiles are not modelled with Cauchy or Gaussian functions) and then are deconvoluted. WA analysis is mainly used to calculate the mean-square strain, while integral breadth methods are used to obtain information of a maximum (upper limit) strain value.

Fourier coefficients of the total intensity are computed using the matrix operator C and the vectorized peaks f, according to

$$\mathbf{A} = \mathbf{C} \cdot f$$

where **C** is the discrete Fourier transform (DFT) transformation matrix. The natural logarithm of the DFT of the normalized intensity can be expressed as

$$\ln A(g^2, L^2) \cong \ln A^S(L) - 2\pi^2 g_{hkl}^2 L^2 \langle \epsilon^2 \rangle$$

This relationship is computed by a linear regression of the coefficients of two reflections of the same family at different values of L. The value of $\langle \epsilon^2 \rangle$ is determined from the absolute value of the slope, while the points at $g^2 = 0$ represent the natural logarithm of the size coefficients A^S.

Statistical distribution: Polycrystalline particles can occur in different sizes and shapes, which both can be described by a statistical distribution using a model that include mainly mean and variance parameters (Langford *et al.*, 2000; Scardi and Leoni, 2001). A initial model can assume the same size (in nm) for particles meaning that the diffracting volume of a specimen is assumed to consist of individual coherently diffracting domains (i.e. crystallites). Such domain is unique or significantly more representative as compared to others. Thus, a corresponding size distribution is not essential for further calculations of integral breadth methods. In this model, it can be also assumed that all the particles are of the same shape (e.g. spherical) into the statistical ensemble and hence, it represent a constant for calculations. For non-spherical particles (e.g. rods, tubes), it can be defined and additional shape parameter (e.g. length, L) to which the Gamma distribution can be employed into the calculations.

Elastic anisotropy: The study the microstructure started for bulk materials. Then, Williamson-Hall (WH) and Warren-Averbach (WA) methods were developed to obtain microstructural information but for several cases, it resulted in the lack of a monotonic behavior, an effect that can be explained by strain anisotropy.

Polycrystalline materials undergo micro-strain as long as these structures contain a large volume fraction of defects. The strain is anisotropic, meaning that unavoidable difficulties appear when using WH and WA methods. For students, the Rietveld method would be computationally more complex for incorporating dislocation models. A scale transformation that accounts for strain anisotropy would effectively decouple the sample's size and strain contributions using the concept of a weight factor to distinguish each dislocation (Wilkens, 1970; Krivoglaz, 1983; Klimanek, 1988). WH and WA methods can be modified with by making use of this concept introducing the calculation of contrast factors, Chkl, (Ungar and Borbely, 1996). Nowadays, the meaning of such factors can be interpreted as the visibility for each dislocation (Armstrong and Lynch, 2004).

THE SET-OF-ROUTINES

Input: It requires a rawdata.dat file containing raw data from experiment. A main file (main.m) is used as input for the following routines:

- Database: cubix.m (file with Miller indices for cubic specimens); instrumental.m (file containing the instrumental function as a quadratic equation).
- Anode: wavelength.m (file with wavelengths for Co, Cu, Mo, Cr, Ni and Fe).
- Background: bkg1st.m (routine for first order background determination) and bkgspline.m (function with a polynomial background routine using Hermite

functions), findmin.n (function to create automatically a database of points for polynomial background determination).

- Smoothing: smoother.m (routine based on).
- $K\alpha_2$ removal: ka2.m (routines based on), bspline.m (file for computation of B-spline basis).
- Peaks: peaksdetection.m (set of routines for peak finding), deriv.m (first derivative of profile line using 2-point central difference), gauss.m (file to fit a peak to a Gaussian and calculate position, width and height). IndexCub do not use the common findpeaks routine from Matlab/Octave.
- Indexing: cell.m (file to determine crystal structure, cell parameters and atomic factor packing for cubic specimens).
- FWHM: fwhm.m (routine based on linear interpolation method).
- Integral breadth: beta.m (function based on the trapezoidal method).
- Size: scherrer.m (function to determine crystallite size).
- Microstructure: iba.m (routine for integral breadth calculations), whall.m (routine for Willamson-Hall calculation), wa.m (for Warren-Averbach calculation).
- Anysotropic: edge.m and screw.m (routines to calculate contrast factors).

Output: Octave GUI interface shows results and calculations for type of cell, average of *a* cell parameter, atomic packing factor, a list of $2\theta_i$ peaks, *hkl* Miller planes, *d* interplanar distance, strain, FWHM and integral breadth values, Williamson-Hall analysis with standard deviation. A graphics for smoother curve, $K\alpha_2$, Williamson-Hall plot, and Warren-Averbach coefficients. For calculations, GNU-Octave requires two main libraries packages, which can be loaded from the command window: pkg load control and pkg load signal.

TEST CASES

After considering appropriate experimental setup for XRD data acquisition, the user can execute the main.m routine to calculate properties of specimens. Here, we tested NaCl, Si, and sputtered Au thin-films. Figure 1 shows results for NaCl. Intensities of raw data, as well as $K\alpha_1$ and $K\alpha_2$ are shown for comparison in two representative peaks. In addition to this, it is observed a strong line broadening due to NaCl are mostly composed by small size crystallites (Fig. 1).

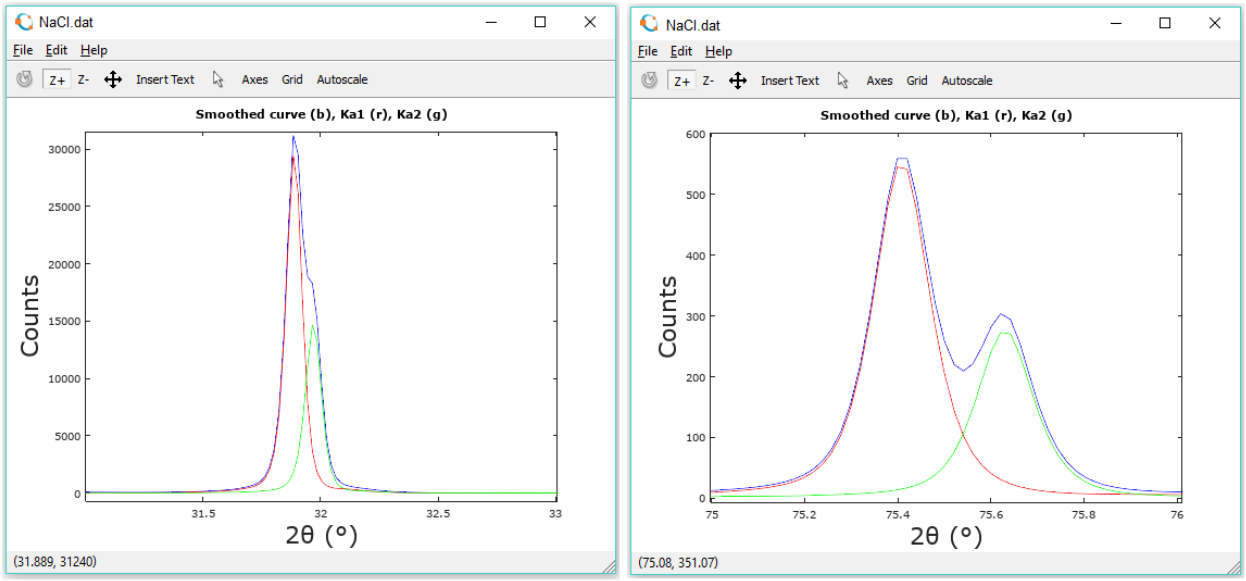

Fig. 1. Integral breadth analysis for NaCl for two representative peaks. The blue line contains the original data points, while the red and green lines represent the separated $K\alpha_1$ and $K\alpha_2$ intensities.

Table 2. NaCl solution: FCC crystal system, $\langle a \rangle$ = 5.6273Å, V = 178.2 Å^3, APF=0.74078.

$2\theta_i$	$h^2+k^2+l^2$	a (Å)	d (Å)	size (nm)
27.56	3	5.6072	1.6667	81.703
31.88	4	5.616	1.4602	107.28
45.61	8	5.6282	1.0793	73.638
56.61	12	5.6346	0.9237	74.512
66.35	16	5.6373	0.8419	102.55
75.39	20	5.6403	0.7969	77.448

Table 3. Si solution: diamond cubic crystal system, system, $\langle a \rangle$ = 5.4112Å, V=158.4 Å^3, APF=0.74078.

$2\theta_i$	$h^2+k^2+l^2$	a (Å)	d (Å)	size (nm)
27.42	3	5.4419	1.6205	86.238
47.28	8	5.4402	1.0498	83.248
56.11	11	5.4397	0.9292	79.88
69.12	16	5.4384	0.8254	79.82
76.36	19	5.4387	0.7936	85.06

The integral breadths (β_{hkl}) of individual *hkl*-reflections were determined and plotted as a function of the projection of diffracting plane normal onto the basal (cross-sectional) plane. From Fig. 2, it is observed that the integral breadth does not depend monotonically for NaCl, but a trend is visible for epitaxial Si. Under such circumstance is important to perform a calculation of contrast factor in NaCl to obtain information of strain through the modified WH or WA methods.

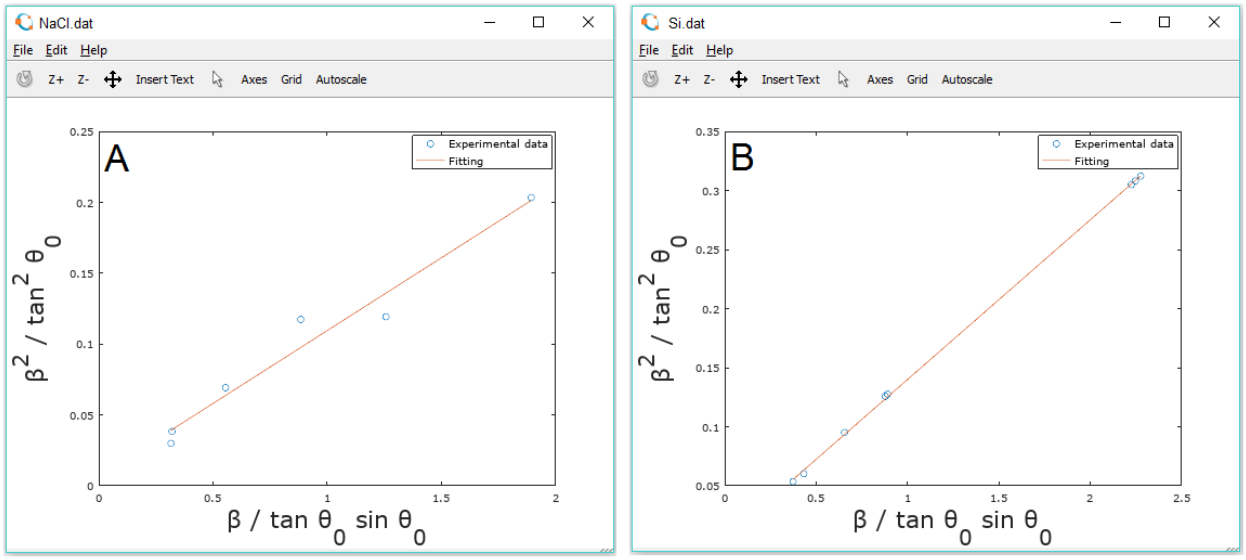

Fig. 2. Integral breadth analysis for NaCl (A) and Si (B). The red lines indicate the linear fitting.

Determination of cell type and peak indexation for Au thin-films are computed using a comparison with a database of cubic crystal structures located in the file cubix.m. Broadening measurements are computed with simple methods: linear interpolation of data for FWHM and integration by trapezoidal method for integral breadth. Crystallite size and lattice strain at zero order are computed using the calculated Integral breadth formula substitution.

Table 4. Au (400 RF) solution: FCC crystal system, system, $\langle a \rangle$ = 5.4112Å, V=158.4 Å^3.

$2\theta_i$	$h^2+k^2+l^2$	size (nm)	strain (%)	FWHM	β
38.0	3	20.2	0.544	0.433	0.541
45.1	4	16.6	0.576	0.541	0.68
64.9	8	19.8	0.341	0.496	0.634
77.8	11	20.5	0.281	0.52	0.657
81.9	12	19.9	0.277	0.551	0.68
97.9	16	16.1	0.298	0.79	0.97

Preliminary diffraction patterns recorded on the Au thin-films indicated a strong preferred orientation in the [111] direction perpendicular to the substrate. After raw data processing, smoothing and Kα_2 removal, the peaks can be separated individually as shown in Figure 3 (right) for a further Warren-Averbach analysis.

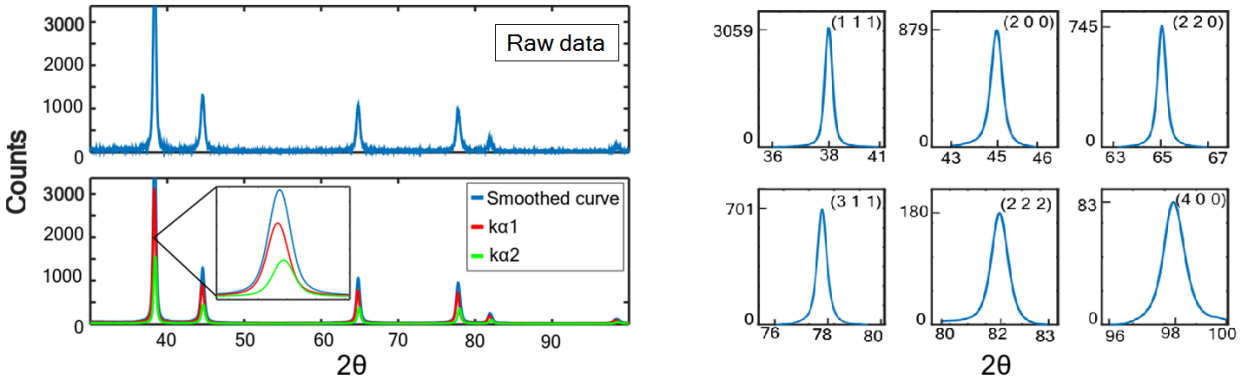

Fig. 3. Diffraction profile (left) and the observed diffracted peaks from Au thin-film (right). The red lines and green lines indicates $K\alpha_1$ and $K\alpha_2$ contributions.

Fourier coefficients of the total intensity are shown in Figure 4A. The natural logarithm of the DFT of the normalized intensity, L, is shown in Figure 4B. In order to compute the mean column length $\langle d \rangle$, the polynomial curve

$$p(x) = (1 - ax - bx^2)\exp(-cx^2)$$

was fitted to the $A^S(L)$ plot, and the calculation of the tangent line yields the value $\langle d \rangle$ at the intersection with the L axis, as shown in Figure 4C.

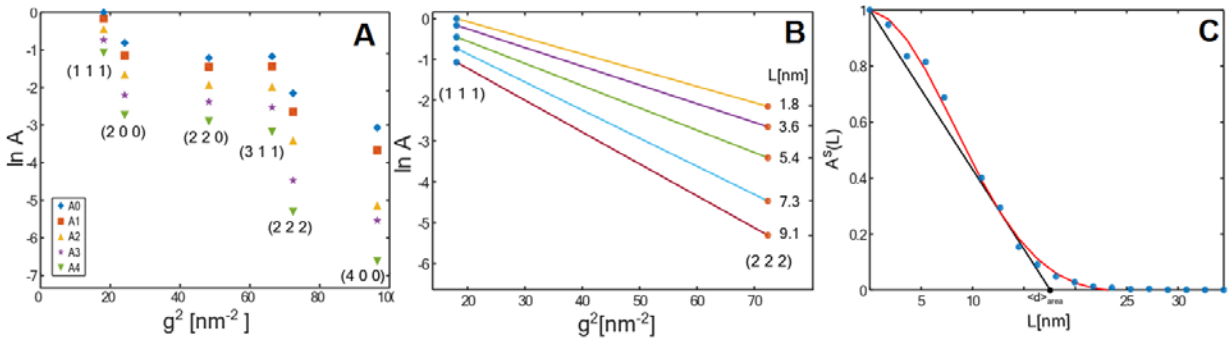

Fig. 4. Warren-Averbach analysis for Au thin-films.

From Figure 4C is observed than the prepared thin-films show a strong texture that may result in coherence of X-rays scattered from adjacent nanocrystallites. In particular, a coherently diffracting domain size of about 17.6 nm was calculated in Au thin-films prepared by RF magnetron sputtering. For the same thin-film, the diffracting domain size was calculated in 28.5 nm when using Bragg-Brentano geometry. This result can be related with the low quality of those obtained diffractograms as well as some basic problems underlying the use of bulk models in thin films system. Due to the small incidence angle (ω<1°), the irradiated area on the film surface is large, therefore the diffracted beam is wide which usually yields several times worse peak profile resolution than in the case of focusing Bragg-Brentano geometry.

The microstructure characterization for systems with strain anisotropy require calculations of contrast factors. A subroutine calculates these values according:

$$\bar{C} = C_{hkl,0}(1 - q\mu H^2)$$

IndexCub allows the selection of a percentage of screw or edge dislocations trough the parameter μ. Computed contrast factors came from routines screw.m and edge.m that are incorporated to extend the WH formalism. Thus, a second order polynomial fit is performed to obtain the function containing deconvoluted size and strain. From diffractograms of Au thin-films, it was calculated 13% and 73% of strain respectively when using line profiles obtained with GIXRD and Bragg-Brentano geometries. The high value from BB indicates that line profile evaluation methods may detect a false microstrain broadening. Several studies confirm a correlation between residual stress, stress-free lattice parameter, microdistortions and the size of coherently diffracting domains, it is also know that the variation in peak shape between samples can lead to severe systematic errors as for instance in the determination of strain percentage from modified WH analysis.

EXPERIMENTAL DETAILS

Powder specimens: NaCl (Sigma-Aldrich) powder sample was prepared by hand-milling in an agate mortar with a further heat treatment performed at 450 °C for 48 h. The powder was deposited on a silicon plate and the diffraction measurement was carried out in a Bruker X-ray D2 Phaser powder diffractometer using Cu-Kα radiation (λ = 0.154 nm; 30 kV, 10 mA), Ni β-filtered and Lynxeye detector. Data were recorded with a step size of 0.002° and an integration time of 2 s from 10° to 100° (2θ).

Thin films: Au thin-films were prepared from PVD methods. Nanocrystallites deposited with different conditions on commercial quartz glass slides were grown using an Intercovamex-V3 sputtering system. X-ray diffraction patterns of thin-films were measured in a diffractometer (PANalytical, Empyrean) using the GIXRD with ω=1° and Bragg-Brentano geometries with CuKα radiation (λ = 0.154 nm; 45 kV, 40 mA), Ni β-filter, and the PIXcel detector (in scanning mode).

Standard sample: Ceramic corundum ($A1_2O_3$) from NIST was used as an instrumental standard to estimate the effect of the instrumental broadening. A measurement of a corundum (Al_2O_3) standard was carried out under analogous conditions of specimens. The measured instrumental function parameters were $a = 8.2\times10^{-2}$, $b = 3\times10^{-4}$ and $c = 8\times10^{-6}$.

CONCLUSIONS

We have described the basis of a ready-to-use set of routines for X-ray line profile analysis, including Williamson-Hall, Warren-Averback and contrast factor calculations. As long as modifications on the state-steady routines were performed, this task lead to a friendly GNU computational approach, which is expected to raise a significant understanding of XLPA in undergraduate students. Future works may include methods especially designed for other structures than cubic materials. In the same way, it is mandatory to increase this property furthermore to allow indexing multiphase patterns as well. It is noteworthy to mention to students that electron microscopy is always the tool for cross-checking XRD results for microstructure analysis.

ACKNOWLEDGEMENTS
We thank to Dr. J. Aguilar for supporting in XRD experiments for Au thin-films, and Dr. R. Cué for preparing Au films. This study was partially supported by the National Council of Science and Technology of Mexico (CONACyT, grant 269399).

REFERENCES

Armstrong, N, Lynch, P. (**2004**). "Determining the dislocation contrast factor for X-ray line profile analysis", in *Diffraction Analysis of the Microstructure of Materials*, edited by E. J. Mittemeijer and P. Scardi (Springer, Heidelberg) pp. 249–286.

Borbély, A., Dragomir-Cernatescu, J., Ribárik, G., Ungár, T. (**2003**). "Computer program ANIZC for the calculation of diffraction contrast factors of dislocations in elastically anisotropic cubic, hexagonal and trigonal crystals," J. Appl. Crystallogr. **36**, 160–162.

Butera, R.A., Waldeck, D.H. (**1997**). "X-ray diffraction investigation of Alloys," J. Chem. Educ. **74**, 115–119.

Cavazos-Cavazos, D., Contreras-Torres, F.F. (**2017**). "Determination of contrast factors for cubic slip-systems and their application in the microstructural characterization of binary Fm 3m materials," J. Phys. Chem. Solids. **110**, 36–42.

Cranswick, L. (**2008**). "Computer software for powder diffraction," in *Powder Diffraction: Theory and Practice*, edited by R. E. Dinnebier and S. J. L. Billinge (RSC Publishing, Cambridge) pp. 494–570.

de Rooi, J.J., van der Pers, N.M., Hendrikx, R.W.A., Delhez, R. A., Böttgerb, J., Eilersa, P.H.C. (**2014**). "Smoothing of X-ray diffraction data and Ka2 elimination using penalized likelihood and the composite link model," J. Appl. Crystallogr. **47**, 852–860.

Eilers, P.H.C. (**2007**). "Ill-posed problems with counts, the composite link model and penalized likelihood," Stat. Model. **7**, 239–254.

Gleiter, H. (**2000**). "Nanostructured materials: basic concepts and microstructure," Acta Mater. **48**, 1–29.

Gubicza, J. (**2014**). *X-Ray Profile Analysis in Materials Science* (IGI Global, Hershey).
Hoff, W.D, Kitchingman, W.J. (**1966**). "Computer indexing of X-ray powder patterns from crystals of unknown structures," J. Sci. Instrum. **43**, 952–953.

Jenkins, R. (**2001**). "Landmarks in the development of powder diffraction instrumentation," J. Chem. Educ. **78**, 601–606.

Klimanek, P., Kuzel, R. (**1988**). "X-ray diffraction line broadening due to dislocations in non-cubic materials. I. General considerations and the case of elastic isotropy applied to hexagonal crystals," J. Appl. Crystallogr. **21**, 59–66.

Kril, C. E., Birringer, R. (**1998**). “Estimating grain-size distributions in nanocrystalline materials from X-ray diffraction profile analysis,” Philos. Mag. A **77**, 621–640.

Krivoglaz, M.A., Martynenko, O.V., Ryaboshapka, K.P. (**1983**). “Effect of dislocation distribution correlation on X-ray diffraction by deformed crystals,” Phys. Metals Metallogr. **55**, 5–17.

Langford, J.I., Louër, D., Scardi, P. (**2000**). “Effect of a crystallite size distribution on X-ray diffraction line profiles and whole-powder-pattern fitting,” J. Appl. Crystallogr. **33**, 964–974.

Leoni, M., Confente, T., Scardi, P. (**2006**). “PM2K: a flexible program implementing Whole Powder Pattern Modelling,” Z. Kristallogr. Suppl **23**, 249–254.

Luo, J., Ying, K., Bai, J. (**2005**). “Savitzky–Golay smoothing and differentiation filter for even number data,” Signal Process. **85**, 1429–1434.

Martinez-Garcia, J., Leoni, M., Scardi P. (2009). “A general approach for determining the diffraction contrast factor of straight-line dislocations,” Acta Crystallogr. A, **65**, 109–119.

Matej, Z., Nichtová, L., Kuzel, R. (**2008**). “Expanding FOX for microstructure analysis,” Mater. Struct. **15**, 46–49.

Mitra, G.B., Misra, N.K. (**1966**). “Background errors in X-ray diffraction parameters,” Brit. J. App. Phys. **17**, 1319–1328.

Pope, C.G. (**1997**). “X-Ray diffraction and the Bragg equation,” J. Chem. Educ. **74**, 129–131.
Rachinger, W.A. (**1948**). “A correction of the a1 a2 doublet in the measurements of widths of X-ray diffraction lines,” J. Sci. Instrum. **25**, 254–255.

Ribárik, G., Ungár, T., Gubicza, J. (**2001**). “MWP-fit: A program for multiple whole profile fitting of diffraction profiles by ab-initio theoretical functions,” J. Appl. Crystallogr. **34**, 669–676.

Ryan, T. (**2001**). “The development of instrumentation for thin-film X-ray diffraction,” J. Chem. Educ. **78**, 613–616.

Savitzky, A., Golay, M.J.E. (**1964**). “Smoothing and differentiation of data by simplified least squares procedures,” Anal. Chem. **36**, 1627–1639.

Scardi, P., Leoni, M. (**1999**). “Fourier modelling of the anisotropic line broadening of X-ray diffraction profiles due to line and plane lattice defects,” J. Appl. Crystallogr. **32**, 671–682.

Scardi, P., Leoni, M. (**2001**). “Diffraction line profiles from polydisperse crystalline systems,” Acta Crystallogr. Sect. A: Found. Crystallogr. **57**, 604–613.

Scardi, P. Leoni, M. (**2002**). “Whole powder pattern modelling,” Acta Crystallogr. A **58**, 190–200.

Schramm, R.E. (**1971**). “Corrections and calculations on a X-ray diffraction line profile: A computer program,” Nat. Bur. Stand. (U.S.), Tech. Note 600.

Simm, T.H., Withers, P.J., Quinta da Fonseca J. (**2016**). “An evaluation of diffraction peak profile analysis (DPPA) methods to study plastically deformed metals,” Mater. Des. **111**, 331–343.

Snyder, R.L., Fiala, J., Bunge, H.J. (**1999**). *Defect and Microstructure Analysis by Diffraction* (Oxford University Press).

Stojilovic, N. (**2018**). “Using Cu Kα1/Kα2 splitting and a powder XRD system to discuss X-ray generation,” J. Chem. Educ. **95**, 598–600.

Suryanarayana, C. (**1995**). “Nanocrystalline materials,” Intern. Mater. Rev. **40**, 41–64.
Ungar, T. (**1969**). “Computer program for x-ray diffraction line profile analysis,” J. Sci. Instrum. **2**, 114–116.

Ungár, T., Borbély, A. (**1996**). “The effect of dislocation contrast on x-ray line broadening: A new approach to line profile analysis,” Appl. Phys. Lett. **69**, 3173–3175.

Werner, P.-E., Eriksson, L., Westdahl, M. (**1985**). “TREOR, a semi-exhaustive trial-and-error powder indexing program for all symmetries,” J. Appl. Crystallogr. **18**, 367–370.

Wilkens, M. (**1970**). “The determination of density and distribution of dislocations in deformed single crystals from broadened X-ray diffraction profiles,” Phys. Status Solidi A **2**, 359–370.